HHS Public Access

Author manuscript

Heart Rhythm. Author manuscript; available in PMC 2016 May 01.

Published in final edited form as:

Heart Rhythm. 2015 May ; 12(5): 1027–1035. doi:10.1016/j.hrthm.2015.01.045.

Remodeling of Stellate Ganglion Neurons following Spatially Targeted Myocardial Infarction: Neuropeptide and Morphologic Changes

Olujimi A. Ajijola, MD, PhD[*,†], **Daigo Yagishita, MD**[*], **Naveen K. Reddy, BS**[*], **Kentaro Yamakawa, MD**[‡], **Marmar Vaseghi, MD, MS, FHRS**[*,†], **Anthony M. Downs, BS**[¶], **Donald B. Hoover, PhD**[¶], **Jeffrey L. Ardell, PhD**[*,†], and **Kalyanam Shivkumar, MD, PhD, FHRS**[*,†]

[*]UCLA Cardiac Arrhythmia Center, University of California-Los Angeles, California

[†]Neurocardiology Research Center of Excellence, University of California-Los Angeles, California

[‡]Department of Cardiac Anesthesia, University of California-Los Angeles, California

[¶]Department of Biomedical Sciences, Center for Inflammation, Infectious Disease, and Immunity, Quillen College of Medicine, East Tennessee State University, Johnson City, Tennessee

Abstract

Background—Myocardial infarction (MI) induces remodeling in stellate ganglion neurons (SGNs).

Objective—We investigated whether infarct site has any impact on the laterality of morphological changes or neuropeptide expression in stellate ganglia.

Methods—Yorkshire pigs underwent left circumflex artery (LCX, n=6) or right coronary artery (RCA, n=6) occlusion, to create left and right-sided MI, respectively (control: n=10). 5±1 weeks post-MI, left and right stellate ganglia (LSG and RSG, respectively) were collected to determine neuronal size, tyrosine hydroxylase (TH) and neuropeptide Y (NPY) immunoreactivity.

Results—Compared to control, LCX and RCA MI increased mean neuronal size in the LSG (451±25μm^2 vs. 650±34μm^2 vs. 577±55 μm^2, respectively, p=0.0012); and RSG (433±22 μm^2 vs. 646±42 μm^2 vs. 530±41μm^2, respectively, p=0.002). TH-immunoreactivity was present in the majority of SGNs. Both LCX and RCA MI were associated with significant decrease in the percentage of TH-negative SGNs; from 2.58±0.2% in controls to 1.26±0.3% and 0.7±0.3% in LCX and RCA MI respectively for LSG (*p*=0.001); and from 3.02±0.4 in controls to 1.36±0.3% and 0.68±0.2% in LCX and RCA MI respectively for RSG (p=0.002). Both TH-negative and TH-

Address for correspondence: Kalyanam Shivkumar MD PhD, UCLA Cardiac Arrhythmia Center, UCLA Health System, David Geffen School of Medicine at UCLA, Suite 660, Westwood Blvd, Los Angeles CA 90095-1679, Phone: 310 206 6433, Fax: 310 794 6492, kshivkumar@mednet.ucla.edu.

Disclosures: None

Conflict of Interest : The authors have no conflicts of interest to disclose.

positive neurons increased in size following LCX and RCA MI. Neuropeptide Y immunoreactivity was also significantly increased by LCX and RCA MI in both ganglia.

Conclusions—Left and right-sided MI equally induced morphologic and neurochemical changes in LSG and RSG neurons, independent of infarct site. These data indicate that afferent signals transduced following MI result in bilateral changes, and provide a rationale for bilateral interventions targeting the sympathetic chain for arrhythmia modulation.

Keywords

Neuropeptide remodeling; Myocardial infarction; Autonomic nervous system; Sympathetic ganglia; Neuronal remodeling

Introduction

Alterations in autonomic nervous system function have been linked to ventricular and atrial arrhythmias[1-3]. Modulation of elements within the cardiac neural hierarchy has been utilized in the management of arrhythmias and the study of ANS function in humans and in animal models[4-7]. Morphologic changes in neurons located in ganglia within and extrinsic to the heart have been reported in association with ischemic and non-ischemic injury to the heart. Neuronal enlargement, nerve sprouting, and enhancement in neural signals have been reported in stellate ganglia in a myocardial infarction (MI) model in canines and rabbits, and in humans[8-10].

In addition, altered neurochemical expression patterns were shown in SGNs in a number of cardiovascular conditions. In a rat non-ischemic model of heart failure (HF), SGNs were shown to undergo trans-differentiation from an adrenergic to a cholinergic phenotype, manifested by an increase in TH-negative (cholinergic) neurons, mediated by gp130 inflammatory cytokines[11]. In addition, low-level vagal stimulation induced an increase in the percentage of TH-negative neurons in canine stellate ganglia[12], the vast majority of which stained positive for choline acetyltransferase (ChAT). These data suggest that under conditions of non-ischemic heart failure, or during chronic vagal stimulation, there is an adrenergic to cholinergic phenotypic switch. Whether ischemic injury to the heart induces similar phenotypic switch is not known.

The pattern of ventricular innervation from the left and right stellate ganglia (LSG and RSG respectively) has been shown in electrical mapping studies to predominate on the posterior and leftward aspect of the ventricles for LSG; and the anterior and rightward aspect of the ventricles for RSG[13, 14]. Whether neuronal remodeling following infarction is greater in the ganglion (LSG vs. RSG) predominantly innervating the damaged myocardial bed remains unknown. This issue is important as it may guide the laterality of interventional strategies aimed at modulating cardiac sympathetic tone, such as cardiac sympathetic denervation following MI[7].

The aim of the present study was two-fold; 1) to determine whether MI is associated with altered stellate ganglion neuronal expression of adrenergic phenotypes and neuropeptides;

and 2) to assess whether stellate ganglion neural remodeling is greatest in the ganglion (LSG vs. RSG) ipsilateral to the area infarcted.

Materials and Methods

Animal model and infarct induction

Animal experimentation was performed with approval from and in accordance with guidelines set by the University of California Institutional Animal Care and Use Committee (IACUC), and The National Institutes of Health Guide for the Care and Use of Laboratory Animals. A total of 22 animals were studied (12 infarcted, and 10 controls).

The MI was induced as previously published[14]. Briefly, animals weighing 77±10lbs (n=12) were sedated with Telazol (8-10mg/kg, intramuscular) and Fentanyl (50-100mcg, intravenous). After intubation, general endotracheal anesthesia was maintained using by inhaled isoflurane (0.8%-1.5%), and analgesia maintained by hourly boluses of fentanyl (50-100 mcg IV). Next, a balloon tipped coronary angioplasty catheter was advanced over a guide-wire to the right coronary artery (RCA, n=6) or left circumflex artery (LCX, n=6). The balloon was inflated to sub-occlusive pressures, and a 10-20mL suspension containing radio-opaque contrast, sterile saline, and 5-7.5mL of polystyrene microspheres (Polybead® 90μm, Polysciences Inc., Warrington, PA, USA) was slowly injected over 3-5 minutes via the angioplasty catheter. ST-segment elevation in inferior or left sided ECG leads confirmed immediate myocardial injury. Ex vivo contrast-enhanced magnetic resonance imaging (CE-MRI) was performed in some animals at 6 weeks post-infarction.

Histologic and Immunohistochemical Studies

Tissue Handling—Stellate ganglia were removed prior to sacrifice, rinsed, and immediately transferred to cold 10% phosphate-buffered formalin (Fisher Scientific, Pittsburgh, PA) for 5-7days, and then to cold 70% ethanol (Sigma-Aldrich, St Louis, MO) until embedding (< 1 week).

Histologic Stains—Neuronal size was determined from Thionin staining (Fisher Scientific, Pittsburgh, PA) using computerized morphometry analysis (Tissue Studio, Definiens Inc., Parsippany, NJ) as previously published[9].

Immunohistochemical Stains—Adrenergic phenotype was quantified using anti-tyrosine hydroxylase (-TH) antibody (1:200 dilution, Abcam, Cat# ab112, Cambridge, MA, USA) and cholinergic phenotype by anti-choline acetyltransferease antibody (1:100 dilution, Abcam, Cat# ab18736, Cambridge, MA, USA), both detected by diaminobenzidine (DAB, Life Technologies, Green Island, NY) per manufacturer's recommended protocol. All neurons present in the slides were counted using computerized image analysis (Aperio ImageScope, Leica Biosystems, Nussloch, GmbH), and considered adrenergic or cholinergic if they demonstrated any level of TH or ChAT immunoreactivity, respectively. Staining and quantification of the groups were performed in a blinded fashion. Neuropeptide Y (NPY) immunoreactivity was quantified using anti-NPY antibodies (1:500 dilution, ImmunoStar, Cat# 22940, Hudson, WI, USA) and developed with ImmPACT VIP peroxidase substrate kit

(Vector) for a constant time of 4 minutes to ensure uniform staining intensity. All slides were digitally scanned, and the electronic images were stored for analysis (Aperio ImageScope, Leica Biosystems, Nussloch, GmbH)[9]. NPY immunoreacitvity was assessed differently compared to the other stains. Quantifications were performed in five 40X-high power fields (hpfs) at the top, bottom, left, right, and center aspects of the slide. Neurons either labeled darkly, faintly, or were completely negative. All neurons were counted and analyzed in these HPFs, however, only those neurons staining darkly were considered NPY immunoreactive, and were quantified as percentage (of darkly stained neurons per slide). Staining and quantification of the groups were performed in a blinded fashion.

Statistical Analyses

Data are reported as means ± standard error (SEM). Normality and homodecasticity were assessed for each dataset. Multi-group comparisons were performed using a two-way analysis of variance (ANOVA) with Tukey-Kramer minimum significant difference (MSD) test. Post-hoc pairwise comparisons when p values < 0.05, were made using a Wilcoxon rank-sum test or Mann-Whitney U Test. For all comparisons, a P value < 0.05 was considered statistically significant.

Results

Myocardial infarction model

Right- and left-sided MIs were created by percutaneous microsphere occlusion of the right coronary artery (RCA) and left circumflex artery (LCX) as shown in Figure 1 (top and middle panels, respectively). The spatial location of the infarcts was confirmed by magnetic resonance imaging, and gross inspection of the hearts upon sacrifice. Representative examples of specific left and right-sided MIs are shown in Figure 1, bottom panel. Occlusion of the RCA resulted in infarction of the right ventricle and inferior septum; however, the predominant mass of the left ventricle was not affected.

MI induces neuronal enlargement in left and right stellate ganglia independent of infarct location

Neuronal size and distribution were quantified by automated analysis of all neurons from thionin-stained ganglia sections. The number of neurons analyzed per slide in the LSG and RSG of controls were 1997±325 and 1149±65 respectively. For LCX MI, those numbers were 1769±367 and 900±101 respectively; and for RCA MI, those numbers were 1550±197 and 616±147, respectively. Neurons in both LSG and RSG were larger in infarct animals than in controls (Figure 2A). Mean LSG neuronal size in controls, LCX and RCA MI subjects were 451±25μm^2 vs. 650±34μm^2 vs. 577±55 μm^2, respectively (anova p=0.0012; CON vs LCX p=0.001, CON vs RCA p=0.015). In RSG, these values were 433±22 μm^2 vs. 646±42 μm^2 vs. 530±41μm^2 for controls, LCX, and RCA animal subjects respectively (anova p=0.002, CON vs LCX p=0.0002, CON vs RCA p=0.04) (Figure 2B). There were no significant differences in neuronal size between LSG and RSG in any of the conditions studied. A histogram demonstrating the distribution of neuronal sizes across the groups is shown in figure 3, for left and right stellate ganglia. It demonstrates a reduction in neuronal

sizes less than 390 μm^2 to 460 μm^2, and an increase in percentage of neurons greater than 544 μm^2 in size in MI animals relative to controls for both ganglia.

Myocardial infarction is associated with adrenergic profile changes in left and right stellate ganglia

Trans-differentiation of neurons from an adrenergic to cholinergic phenotype has been reported in the heart failure model[11], however, whether an ischemic infarct model exhibits such phenomena remained unknown. We performed tyrosine hydroxylase immunostaining of left and right stellate ganglia from controls, LCX and RCA infarcts. Per slide, an average of 2149±347, 1304±332, and 2389±375 neurons were counted in the LSG of control, LCX MI and RCA MI respectively. In the RSG, the average number of neurons counted per slide was 1648±117, 817± 117, and 1654±369 respectively for control, LCX MI and RCA MI respectively. We measured the percentage of TH-negative neurons, and surprisingly observed a decrease, rather than an increase (Figure 4A) as was previously reported in heart failure. Specifically, the percentage of TH-negative (non-adrenergic neurons) in LSG decreased from 2.58±0.2% in controls to 1.26±0.3% and 0.7±0.3% in LCX and RCA MI respectively for LSG (p=0.001); and from 3.02±0.4 in controls to 1.36±0.3% and 0.68±0.2% in LCX and RCA MI respectively for RSG (p=0.004). (Figure 4B). Results of pairwise comparisons are also presented in Figure 4B. Across the population of animals studied, the intensity of tyrosine hydroxylase staining was greater in both LCX and RCA MI animals than in controls (Figure 4A).

In a subset of animals (n=3), we performed immunostaining of adjacent 4μm thick sections from the same ganglion with TH and choline-actyltransferase (ChAT) a marker of cholinergic neurons. This demonstrated that all TH-negative neurons stained for ChAT (Figure 4C, thick black arrows). As shown in the same figure, a small population of neurons (identified by arrowheads) stained for both TH and ChAT.

Next we examined whether the population of neurons demonstrating enlargement following MI were predominantly of the adrenergic or non-adrenergic phenotype. In control animals, the mean neuronal size of non-adrenergic neurons was significantly greater than adrenergic neurons (Figure 5)(485±21 μm^2 vs. 399±13 μm^2, respectively, p=0.001). Following LCX and RCA MI both neuronal subclasses increased in size, to 679±42 μm^2 and 558±70 μm^2 (p=0.006) respectively for non-adrenergic neurons; and to 616±31 μm^2 and 548±20 μm^2 (p=0.001) (Figure 5) respectively for adrenergic neurons.

Neuropeptide Y immunoreactivity is increased following myocardial infarction

NPY, an adrenergic neuropeptide, has been implicated in a number of cardiovascular processes including regulation of vascular tone, remodeling, and metabolism following exposure to stress[15]. NPY immunoreactivity was assessed as described in representative left and right stellate ganglia sections from control, LCX and RCA-infarcted animal subjects. Across the five 40X high power fields analyzed, an average of 154±10 and 166±12 neurons in LSG and RSG respectively were analyzed in controls, 147±9 and 170±9 neurons respectively, in LCX MI; and 153±18 and 164±9 neurons respectively, in RCA MI. In control ganglia, approximately half of the neurons assessed in both ganglia stained darkly

positive for NPY (40±0.9% and 46±2.5%) for LSG and RSG, respectively. In ganglia from MI subjects, NPY immunoreactivity was significantly increased; (Figure 6A) 72±1.6% ($p<.001$) and 68±2% ($p=0.002$) for LCX and RCA MI respectively in the LSG; and (69±4% ($p=0.002$) and 73±2.4% ($p=0.002$) for LCX and RCA MI respectively in the RSG (anova p values were 0.0004 and 0.006 when comparing the three conditions for LSG and RSG respectively (Figure 6B).

Discussion

Major Findings

The major findings of the present study are 1) post-infarction neuronal enlargement in LSG and RSG is independent of the spatial location of MI (left vs. right); 2) MI is associated with neurochemical remodeling of SGNs, with an increase in neuronal adrenergic phenotype and neuropeptide Y immunoreactive neurons observed; 3) morphologic enlargement of neurons is seen in both adrenergic and non-adrenergic (cholinergic) neurons following myocardial infarction.

Neuronal morphologic changes in cardiomyopathy

Morphologic changes in SGNs have predominantly been studied in the ischemic cardiomyopathy model, with infarction occurring in the left anterior descending coronary artery[8, 16], and a predominant focus on the LSG[9]. However, both stellate ganglia may remodel following MI[10], and further, such remodeling may be different. The findings of the present study indicate that both left and right-sided MI induce morphologic changes in both stellate ganglia, with no relationship to infarct laterality. Stellate ganglion stimulation and measurement of electrophysiological indices (based on regions with greatest response to stimulation) show that innervation from the LSG predominate on the posterior and leftward aspect of the ventricles; and conversely on the anterior and rightward aspect of the ventricles for RSG[13, 14, 17]. The lack of regionality in neural remodeling from left and right-sided MI may reflect a difference in how afferent (transduction of signals following an MI) and efferent sympathetic activation reach the heart. A more important explanation is that the intrinsic cardiac network (ICN)[18] is the primary site transducing cardiac injury to the CNS, and subsequent distribution of remodeling-inducing signals to both stellate ganglia[19, 20] via increased sympathetic outflow. Whether there is differential remodeling in the ICN to left and right-sided MI remains unknown. Another important mechanism for these morphological changes is the hemodynamic impact of MI, activation of cardiovascular[21], renal[22], and intra-thoracic afferents, and subsequent increase in efferent sympathetic signals to the heart via the sympathetic chain. As a result of the enhanced electrophysiologic and metabolic activity, SGNs exhibit the morphological changes identified.

Analyses of the size distribution in stellate ganglia demonstrate that not all neurons enlarge following MI, however, a population of neurons exhibit morphological changes (Figure 3), as has been reported in other models[9]. These neurons may represent efferent and/or local circuit neurons involved in cardiovascular (or cardiopulmonary) regulation, while the unchanged neurons may mediate neurotransmission for other thoracic structures and upper extremity visceral innervation (e.g. sudomotor cholinergic neurons). This hypothesis does

not preclude functional remodeling of certain neuronal populations without morphologic changes.

These data have important implications for the use of cardiac sympathetic denervation in managing refractory ventricular arrhythmias in humans[24]. Unilateral or bilateral removal of a portion of the sympathetic chain (lower half of the stellate ganglion, and T2-T4) is a subject of debate [4, 5, 7]. Physical and functional remodeling of SGNs removed from patients has been reported[9]. Removal of these elements and prevention of further remodeling, along with interruption of afferent and efferent neurotransmission may be mechanism of the beneficial effects seen with this procedure. Removal of unilateral thoracic sympathetic chain, and incomplete mitigation of neural remodeling and neurotransmission at the level of the stellate ganglia may account for the poorer outcomes seen with unilateral vs. bilateral sympathectomy[7].

Neurochemical remodeling of stellate ganglion neurons

Phenotypic trans-differentiation of adrenergic to cholinergic neurons has been demonstrated as a feature of non-ischemic (hypertensive) heart failure in a rat model, mediated by gp130 cytokines enhanced by the heart failure state[11]. Interestingly, a similar phenomenon was reported following chronic low-level vagal stimulation[12]. In the former study, Kanazawa et al. demonstrate a protective effect of adrenergic to cholinergic transdfferentiation in hypoxic conditions. In the latter study, Shen et al demonstrate reduced atrial tachyarrhythmias with low-level vagal nerve stimulation. The findings of the present study however, indicate that ischemic injury to the heart induces a different phenotypic manifestation, where an increase in adrenergic neurons are observed. Although this study assessed one time point, these data suggest a cholinergic to adrenergic neurotransmitter switch, likely reflective of a hyper-adrenergic post-infarct state. Along with this finding, NPY expression was also increased.

Mechanisms that may explain the phenotypic change observed in this study include increased afferent signals to the cardiac neural axis, including the central nervous system, with increased efferent sympathetic outflow to the sympathetic chain, intrinsic cardiac network, and the heart. Another possible mechanism is elevated NGF expression in the heart following MI [8, 25] and by mechanisms of retrograde axonal transport[25, 26], to the stellate ganglia, NGF induces increased expression of adrenergic neurotransmitter.

Despite the change in adrenergic phenotype following left and right-sided MI, both neuronal subtypes demonstrated enlargement following MI. Further, the difference in size between adrenergic and non-adrenergic SGNs observed in controls was lost with the introduction of MI (both LCX and RCA models), as no significant differences in size were seen between adrenergic and non-adrenergic neurons in MI animals. Consistent with morphologic data, this suggests, an overall hyperadrenergic state following MI, the result of which is increased expression of adrenergic neuronal properties. Post-natal changes in neurochemical expression is poorly understood and complex[27], however, it is likely critical for the maintenance of neural plasticity. Changes may be driven by the target tissue, cellular environment, or circulating cytokines including the gp130 class[11]. These changes likely act to maintain longer-term adaptations to the organisms nervous needs. In the heart failure state, adrenergic to cholinergic transdifferentiation may act to decrease sympathetic tone,

and in the case of our study, the increase in expression of adrenergic markers may maintain the hyperadrenergic state.

The multifaceted role of NPY in a variety of cardiovascular or neuro-hormonal conditions remains under intense study. NPY is abundant in the heart in association with sympathetic nerve terminals. In addition to mediating vasoconstriction, it is implicated in the development of hypertension, left ventricular hypertrophy (LVH)[28], and is significantly elevated under chronic cardiac ischemia[29]. It potentiates the effect of norepinephrine and angiotensin[30]. NPY mediates sympathetic-parasympathetic cross talk[31], and has also been shown to diminish parasympathetic neurotransmission in the heart[32]. The expression of NPY in control animals in our study closely matches the range demonstrated by Happola et al in porcine[33]. Consistent with our findings, NPY levels were greater in superior cervical ganglia neurons of rats with hypertension compared to controls[34], as the immunoreactivity with age did not decrease in hypertensive animals as it did in control subjects. NPY expression and regulation is in part under the influence of preganglionic efferent sympathetic signaling[35], suggesting that a possible mechanism for the observed increased NPY expression (and increased TH expression in neurons) in our model is increased post-MI afferent neurotransmission, with resultant efferent sympathetic signaling. Although it is remains unknown what the consequence of increased NPY expression in stellate ganglia is on cardiac NPY expression, and electrophysiology, multiple lines of evidence described above suggest an adverse effect. The increase in NPY, concomitant with increase adrenergic phenotypes in this post-infarct model all point to the increased sympathetic state.

Conclusion

In summary, we present data that both left and right stellate ganglia remodel morphologically and neurochemically following spatially targeted left and right-sided MI that distributed in the innervation territories of the LSG and RSG, respectively. There was no relationship between the degree of morphologic or neuropeptide remodeling in either stellate ganglion, and the laterality of infarction. Non-adrenergic (cholinergic) and adrenergic neurons demonstrate morphologic changes in both ganglia. Lastly, expression of NPY, a sympathetic neuropeptide, was increased in stellate ganglion neurons following both left and right-sided MI. Taken together, these data suggest that myocardial infarction is “sensed” equally by both sides of the cardiac neuraxis, and results in increased bilateral expression of adrenergic markers. A major implication of these data is that bilateral cardiac sympathetic denervation is preferred over unilateral, in the mitigation of stellate ganglion morphologic and neuropeptide remodeling, and cardiac neurotransmission.

Acknowledgments

The authors would like to thank Eileen So, Jaspreet Singh, Jonathan Pang, Tayler Rodriguez, and Emma Kurihara for excellent technical assistance. This study was supported by an A. P. Giannini Post-Doctoral Award to OAA, NIH GM107949 to DBH, and NHLBI R01HL084261 to KS.

References

1. Schwartz PJ. Cardiac sympathetic denervation to prevent life-threatening arrhythmias. Nature reviews Cardiology. 2014; 11:346–353.

2. Shen MJ, Zipes DP. Role of the autonomic nervous system in modulating cardiac arrhythmias. Circulation Research. 2014; 114:1004–1021. [PubMed: 24625726]

3. Vaseghi M, Shivkumar K. The role of the autonomic nervous system in sudden cardiac death. Prog Cardiovasc Dis. 2008; 50:404–419. [PubMed: 18474284]

4. Bourke T, Vaseghi M, Michowitz Y, Sankhla V, Shah M, Swapna N, Boyle NG, Mahajan A, Narasimhan C, Lokhandwala Y, Shivkumar K. Neuraxial modulation for refractory ventricular arrhythmias: value of thoracic epidural anesthesia and surgical left cardiac sympathetic denervation. Circulation. 2010; 121:2255–2262. [PubMed: 20479150]

5. Ajijola OA, Lellouche N, Bourke T, Tung R, Ahn S, Mahajan A, Shivkumar K. Bilateral Cardiac Sympathetic Denervation for the Management of Electrical Storm. J Am Coll Cardiol. 2012; 59:91–92. [PubMed: 22192676]

6. Schwartz PJ, Billman GE, Stone HL. Autonomic mechanisms in ventricular fibrillation induced by myocardial ischemia during exercise in dogs with healed myocardial infarction. An experimental preparation for sudden cardiac death. Circulation. 1984; 69:790–800. [PubMed: 6697463]

7. Vaseghi M, Gima J, Kanaan C, Ajijola OA, Marmureanu A, Mahajan A, Shivkumar K. Cardiac sympathetic denervation in patients with refractory ventricular arrhythmias or electrical storm: intermediate and long-term follow-up. Heart rhythm. 2014; 11:360–366. [PubMed: 24291775]

8. Han S, Kobayashi K, Joung B, Piccirillo G, Maruyama M, Vinters H. Electroanatomical remodeling of the left stellate ganglion after myocardial infarction. J Am Coll Cardiol. 2012; 59:954–61. [PubMed: 22381432]

9. Ajijola OA, Wisco JJ, Lambert HW, Mahajan A, Stark E, Fishbein MC, Shivkumar K. Extracardiac neural remodeling in humans with cardiomyopathy. Circ Arrhythm Electrophysiol. 2012; 5:1010–1116. [PubMed: 22923270]

10. Nguyen BL, Li H, Fishbein MC, Lin SF, Gaudio C, Chen PS, Chen LS. Acute myocardial infarction induces bilateral stellate ganglia neural remodeling in rabbits. Cardiovasc Pathol. 2012; 21:143–8. [PubMed: 22001051]

11. Kanazawa H, Ieda M, Kimura K, et al. Heart failure causes cholinergic transdifferentiation of cardiac sympathetic nerves via gp130-signaling cytokines in rodents. J ClinInvest. 2010; 120:408–421.

12. Shen MJ, Shinohara T, Park HW, et al. Continuous low-level vagus nerve stimulation reduces stellate ganglion nerve activity and paroxysmal atrial tachyarrhythmias in ambulatory canines. Circulation. 2011; 123:2204–2212. [PubMed: 21555706]

13. Yanowitz F, Preston JB, Abildskov JA. Functional distribution of right and left stellate innervation to the ventricles. Production of neurogenic electrocardiographic changes by unilateral alteration of sympathetic tone. Circ Res. 1966; 18:416–428. [PubMed: 4952701]

14. Ajijola OA, Yagishita D, Patel KJ, Vaseghi M, Zhou W, Yamakawa K, So E, Lux RL, Mahajan A, Shivkumar K. Focal myocardial infarction induces global remodeling of cardiac sympathetic innervation: neural remodeling in a spatial context. Am J Physiol Heart Circ Physiol. 2013; 305:H1031–1040. [PubMed: 23893167]

15. Abe K, Tilan JU, Zukowska Z. NPY and NPY receptors in vascular remodeling. Curr Top Med Chem. 2007; 7:1704–1709. [PubMed: 17979779]

16. Zhou S, Jung BC, Tan AY, Trang VQ, Gholmieh G, Han SW, Lin SF, Fishbein MC, Chen PS, Chen LS. Spontaneous stellate ganglion nerve activity and ventricular arrhythmia in a canine model of sudden death. Heart Rhythm. 2008; 5:131–139. [PubMed: 18055272]

17. Vaseghi M, Yamakawa K, Sinha A, So EL, Zhou W, Ajijola OA, Lux RL, Laks M, Shivkumar K, Mahajan A. Modulation of regional dispersion of repolarization and T-peak to T-end interval by the right and left stellate ganglia. Am J Physiol Heart Circ Physiol. 2013; 305:H1020–1030. [PubMed: 23893168]

18. Armour JA. The little brain on the heart. Cleve Clin J Med. 2007; 74(Suppl 1):S48–51. [PubMed: 17455544]

19. Beaumont E, Salavatian S, Southerland EM, Vinet A, Jacquemet V, Armour JA, Ardell JL. Network interactions within the canine intrinsic cardiac nervous system: implications for reflex control of regional cardiac function. The J Physiol. 2013; 591:4515–4533.

20. Hardwick JC, Ryan SE, Beaumont E, Ardell JL, Southerland EM. Dynamic remodeling of the guinea pig intrinsic cardiac plexus induced by chronic myocardial infarction. Auton Neurosci. 2013
21. Wang HJ, Wang W, Cornish KG, Rozanski GJ, Zucker IH. Cardiac sympathetic afferent denervation attenuates cardiac remodeling and improves cardiovascular dysfunction in rats with heart failure. Hypertension. 2014; 64:745–755. [PubMed: 24980663]
22. Hou Y, Hu J, Po SS, Wang H, Zhang L, Zhang F, Wang K, Zhou Q. Catheter-based renal sympathetic denervation significantly inhibits atrial fibrillation induced by electrical stimulation of the left stellate ganglion and rapid atrial pacing. PLoS One. 2013; 8:e78218. [PubMed: 24223140]
23. Evans RG, Ludbrook J, Michalicek J. Characteristics of cardiovascular reflexes originating from 5-HT3 receptors in the heart and lungs of unanaesthetized rabbits. Clin Exp Pharmacol Physiol. 1990; 17:665–679. [PubMed: 2279353]
24. Ajijola OA, Vaseghi M, Mahajan A, Shivkumar K. Bilateral cardiac sympathetic denervation: why, who and when? Expert Rev Cardiovasc Ther. Aug.2012 10:947–949. [PubMed: 23030281]
25. Zhou S, Chen LS, Miyauchi Y, Miyauchi M, Kar S, Kangavari S, Fishbein MC, Sharifi B, Chen PS. Mechanisms of cardiac nerve sprouting after myocardial infarction in dogs. Circ Res. 2004; 95:76–83. [PubMed: 15166093]
26. Ajijola OA, Shivkumar K. Neural remodeling and myocardial infarction: the stellate ganglion as a double agent. Journal of the American College of Cardiology. 2012; 59:962–964. [PubMed: 22381433]
27. Apostolova G, Dechant G. Development of neurotransmitter phenotypes in sympathetic neurons. Auton Neurosci. 2009; 151:30–38. [PubMed: 19734109]
28. McDermott BJ, Bell D. NPY and cardiac diseases. Curr Top Med Chem. 2007; 7:1692–1703. [PubMed: 17979778]
29. Cuculi F, Herring N, De Caterina AR, Banning AP, Prendergast BD, Forfar JC, Choudhury RP, Channon KM, Kharbanda RK. Relationship of plasma neuropeptide Y with angiographic, electrocardiographic and coronary physiology indices of reperfusion during ST elevation myocardial infarction. Heart. 2013; 99:1198–1203. [PubMed: 23403409]
30. Edvinsson L, Ekblad E, Hakanson R, Wahlestedt C. Neuropeptide Y potentiates the effect of various vasoconstrictor agents on rabbit blood vessels. Br J Pharmacol. 1984; 83:519–525. [PubMed: 6593107]
31. Shanks J, Herring N. Peripheral cardiac sympathetic hyperactivity in cardiovascular disease: role of neuropeptides. Am J Physiol Regul Integr Comp Physiol. 2013; 305:R1411–1420. [PubMed: 24005254]
32. Smith-White MA, Iismaa TP, Potter EK. Galanin and neuropeptide Y reduce cholinergic transmission in the heart of the anaesthetised mouse. Br J Pharmacol. 2003; 140:170–178. [PubMed: 12967946]
33. Happola O, Lakomy M, Majewski M, Wasowicz K, Yanaihara N. Distribution of neuropeptides in the porcine stellate ganglion. Cell Tissue Res. 1993; 274:181–187. [PubMed: 7694801]
34. Gurusinghe CJ, Harris PJ, Abbott DF, Bell C. Neuropeptide Y in rat sympathetic neurons is altered by genetic hypertension and by age. Hypertension. 1990; 16:63–71. [PubMed: 2365447]
35. Hanze J, Kummer W, Haass M, Lang RE. Neuropeptide Y mRNA regulation in rat sympathetic ganglia: effect of reserpine. Neurosci Lett. 1991; 124:119–121. [PubMed: 1713314]

Glossary of Abbreviations

ANOVA	Analysis of Variance
ANS	Autonomic Nervous System
CE-MRI	Contrast Enhanced-Magnetic Resonance Imaging
ChAT	Choline Acetyltransferase

CON	Control
ECG	Electrocardiogram
HF	Heart Failure
ICN	Intrinsic Cardiac Network
LCX	Left Circuflex Coronary Artery
LSG	Left Stellate Ganglion
LVH	Left Ventricular Hypertrophy
MI	Myocardial Infarction
NGF	Nerve Growth Factor
NPY	Neuropeptide Y
RCA	Right Coronary Artery
RSG	Right Stellate Ganglion
SD	Standard Deviation
SEM	Standard Error of The Mean
SGN	Stellate Ganglion Neuron(s)
TH	Tyrosine Hydroxylase

Clinical Perspectives

In this manuscript, we present evidence that post-infarction morphologic and neurochemical remodeling of the left and right stellate ganglia is independent of the location of the infarction (left- or right-sided infarct). We also identified increased relative expression of tyrosine hydroxylase in stellate ganglion neurons, in association with increased expression of neuropeptide Y. As post-infarction adrenergic signaling has been linked to arrhythmogenesis, neuronal increased adrenergic expression is a novel target in the mitigation of the hyper-adrenergic state. Further studies to identify the key elements driving adrenergic expression in neurons may elucidate pharmacologic or interventional therapies to prevent arrhythmias induced by increased adrenergic signaling.

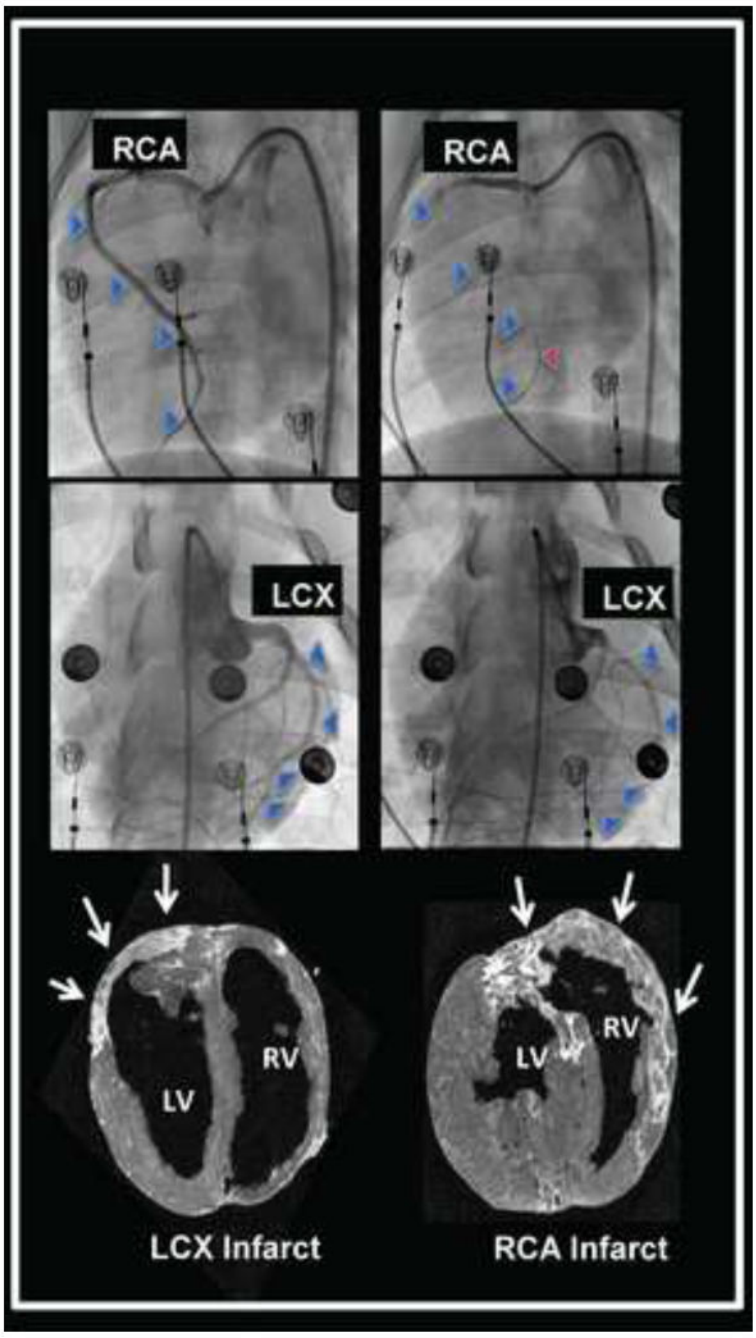

FIGURE 1. Myocardial Infarct Models

Angiographic evidence of occlusion of the right coronary artery (RCA) and left circumflex artery (LCX) to create right and left-sided myocardial infarctions are shown in the **top** and **middle** panels, respectively. The blue arrowheads trace the course of the vessel at baseline, and indicate the missing vessel following microsphere occlusion. The red arrowhead identifies an intracoronary guidewire tracing out the course of the occluded RCA. The **bottom** panel shows delayed gadolinium magnetic resonance images of the RCA and LCX

infarcts (bright tissue), also identified by white arrows. Short axis images of the ventricles are presented, viewed from the apex of the heart.

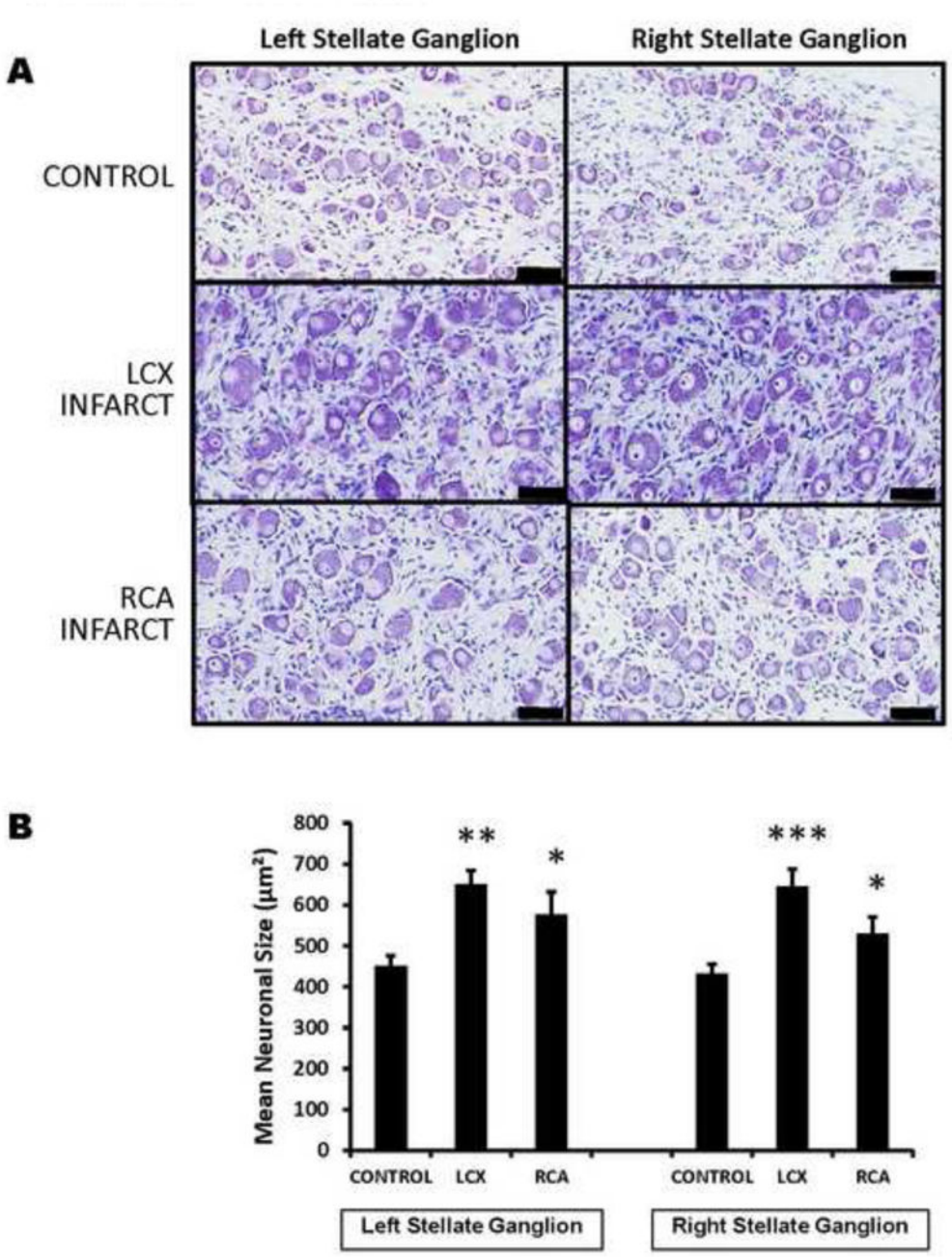

FIGURE 2. Myocardial Infarction Induces Stellate Neuronal Enlargement Without Relationship To Laterality

A. Shown are representative images of thionin-stained sections of right and left stellate ganglia from control animals, compared to left circumflex (LCX) artery and right coronary artery (RCA) occlusions to create left and right-sided myocardial infarctions. The larger neurons in LCX and RCA infarcts can be visually appreciated. (scale bar 50μm). **B.** Quantification of mean neuronal size in left and right stellate ganglia of control subjects

compared to LCX and RCA infarcts are presented. *p<0.05, ** p<0.01, ***P<0.001 when compared to controls.

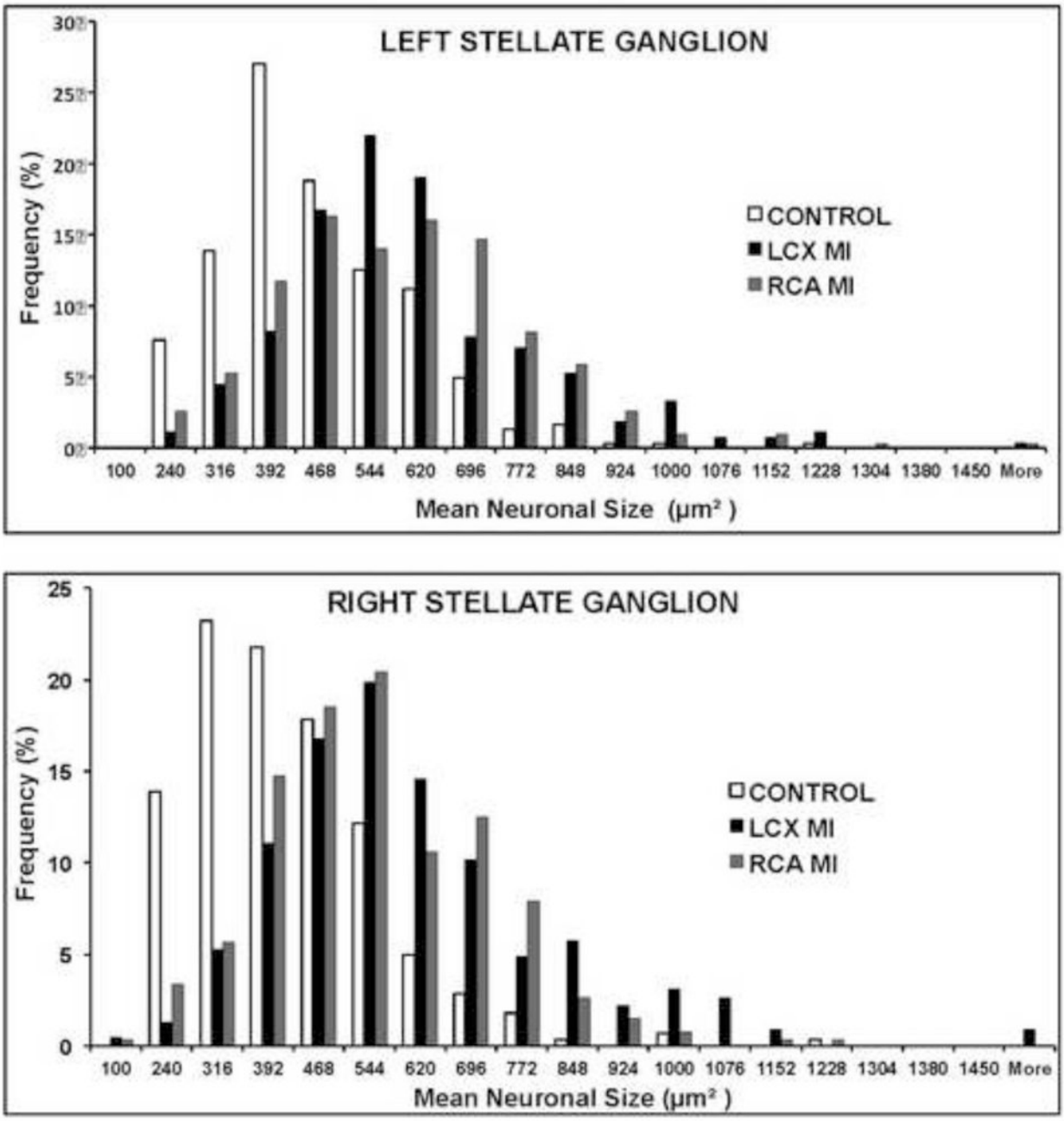

FIGURE 3. Distribution Of Stellate Ganglion Neuronal Size By Ganglion And Infarct Site

Histograms of neuronal size distribution from left and right stellate ganglia (LSG and RSG, respectively) from control animals subjects, and left circumflex (LCX) and right coronary artery (RCA) infarcts, creating left and right-sided infarcts respectively.

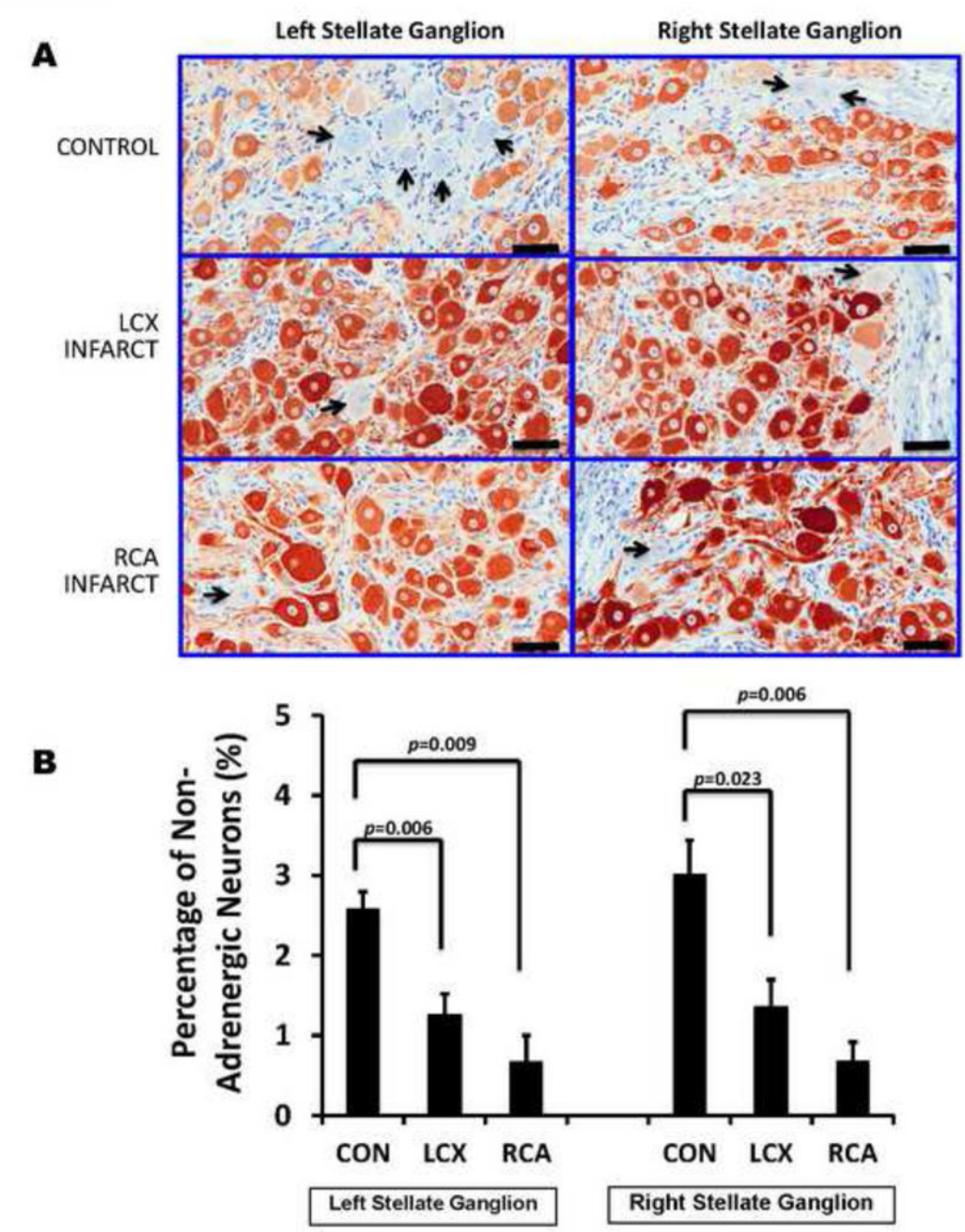

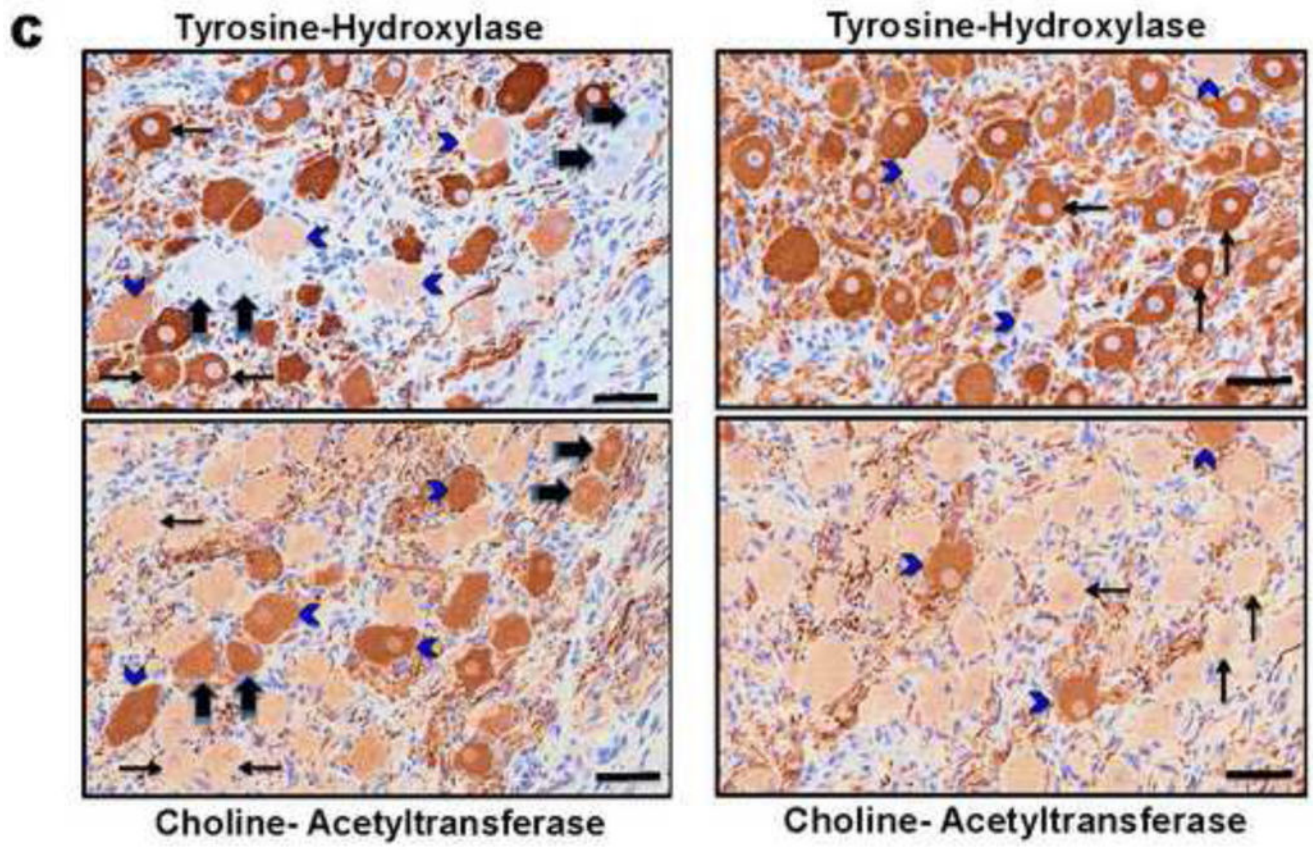

FIGURE 4. Myocardial Infarction Induces Neurochemical Remodeling Of Stellate Ganglion Neurons

A. Representative tyrosine hydroxylase (TH)-stained sections of right and left stellate ganglia from control animals, compared to left circumflex (LCX) artery and right coronary artery (RCA) occlusions to create left and right-sided myocardial infarctions. More TH negative neurons (indicated by black arrows)can be appreciated in control, compared to LCX and RCA infarcts. Larger neurons in infarcted ganglia can also be appreciated. Scale bar = 50μm. **B.** Quantification of the percentage of TH-negative neurons in left and right stellate ganglia of control subjects compared to LCX and RCA infarcts are presented. **C.** Examples of adjacent 4μm sections from a control animal (left panel) and LCX MI animal (right panel) stained with TH, and choline-acetyl transferase (ChAT) demonstrating neurons that stain only for TH (thin black arrows), only for ChAT (thick black arrows) or both (blue arrowheads), although these neurons stain less intensely for TH. Scale bar = 50μm.

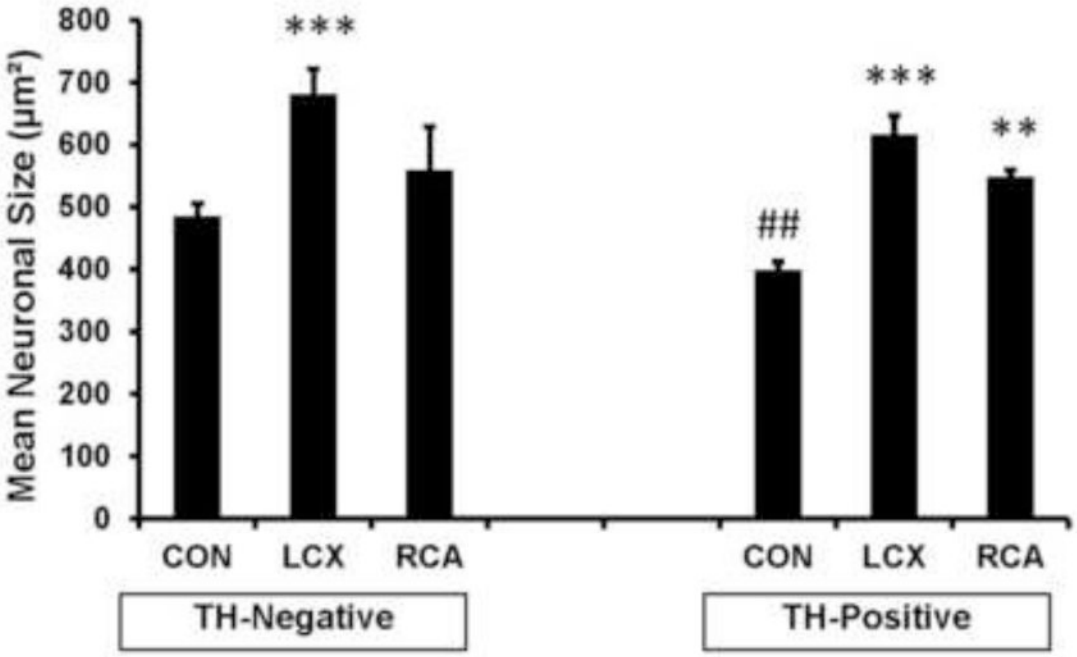

FIGURE 5. Adrenergic and Non-Adrenergic Neurons Enlarge Following Myocardial Infarction

Graphical representation of mean neuronal size of tyrosine hydroxylase (TH) negative and positive neurons in ganglia from control subjects compared to LCX and RCA infarcts are presented. In control animals, TH positive neurons are smaller than TH-negative neurons. Not only are both populations of neurons larger in infarcted animals, the size difference seen in controls is lost. **p<0.01, ***P<0.001 compared to conrol. $^{\#\#}$p<0.01 for Control TH-negative vs Control TH-positive.

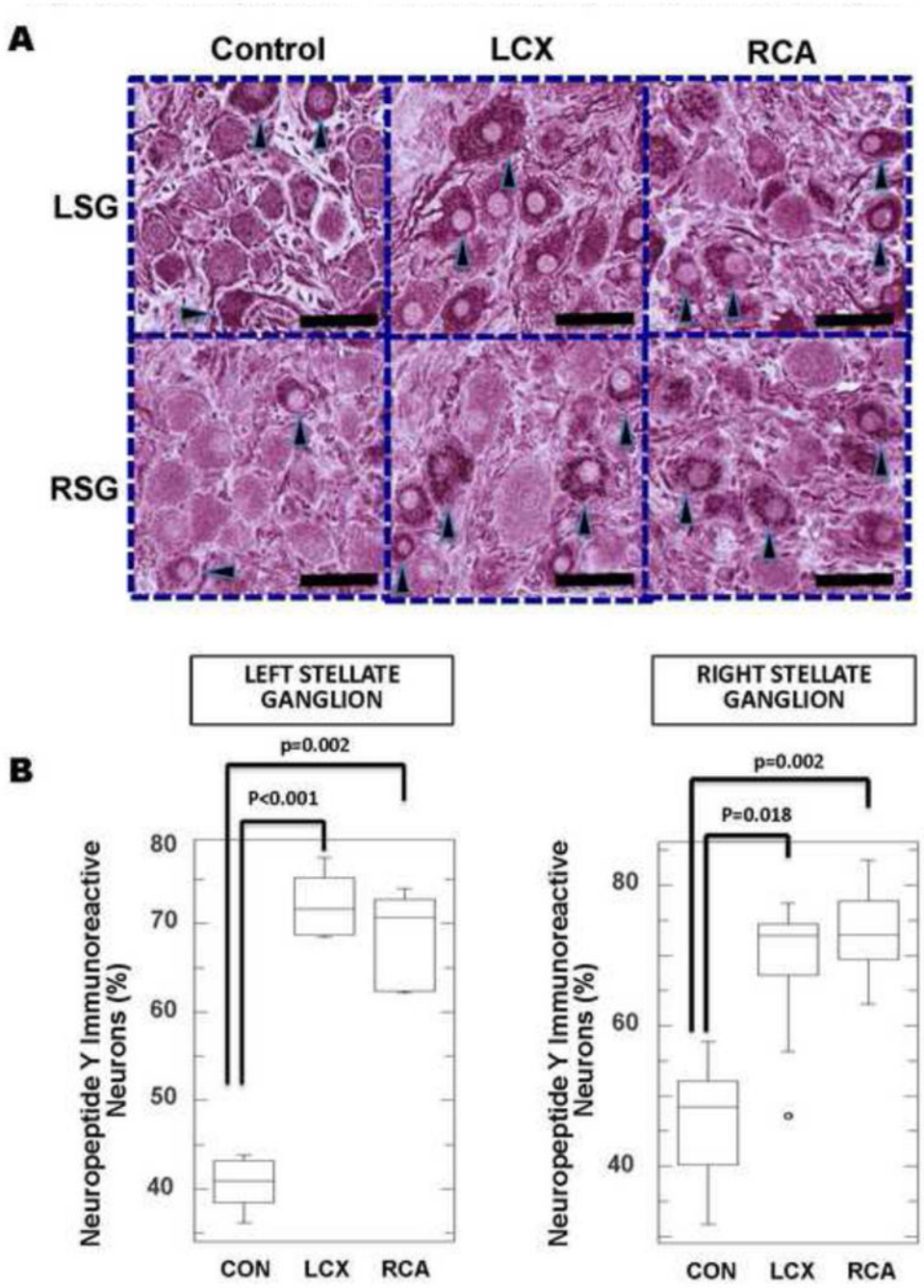

FIGURE 6. Neuropeptide Y immunoreactivity increases following MI

A. Representative neuropeptide Y (NPY)-stained sections of left and right stellate ganglia (LSG and RSG, respectively) from control animals, compared to left circumflex (LCX) artery and right coronary artery (RCA) occlusions to create left and right-sided myocardial infarctions. Increased NPY immunoreactivity in LCX and RCA neurons can be identified. Darkly stained neurons are indicated by black arrow heads. Larger neurons in infarcted ganglia can also be appreciated. Scale bar = 50μm. **B.** Quantification of NPY

immunoreactivity in left and right stellate ganglia of control subjects compared to LCX and RCA infarcts.